Chapter 17

Void Fractions in Two-Phase Flows

Summary: The void fraction ε is one of the most important parameters used to characterize two-phase flows. It is the key physical value for determining numerous other important parameters, such as the two-phase density and the two-phase viscosity, for obtaining the relative average velocity of the two phases, and is of fundamental importance in models for predicting flow pattern transitions, heat transfer and pressure drop. In this chapter, the basic theory and prediction methods for two-phase flows in vertical and horizontal channels and over tube bundles are presented.

17.1 Introduction

Various geometric definitions are used for specifying the void fraction: local, chordal, cross-sectional and volumetric, which are represented schematically in Figure 17.1. The *local* void fraction ε_{local} refers to that at a point (or very small volume when measured experimentally) and thus $\varepsilon_{local} = 0$ when liquid is present and $\varepsilon_{local} = 1$ when vapor is present. Typically, the local time-averaged void fraction is cited, or measured using a miniature probe, which represents the fraction of time vapor, was present at that location in the two-phase flow. If $P_k(r,t)$ represents the local instantaneous presence of vapor or not at some radius r from the channel center at time t, then $P_k(r,t) = 1$ when vapor is present and $P_k(r,t) = 0$ when liquid is present. Thus, the local time-averaged void fraction is defined as

$$\varepsilon_{local}(r,t) = \frac{1}{t}\int_t P_k(r,t)dt \qquad [17.1.1]$$

The *chordal* void fraction $\varepsilon_{chordal}$ is typically measured by shining a narrow radioactive beam through a channel with a two-phase flow inside, calibrating its different absorptions by the vapor and liquid phases, and then measuring the intensity of the beam on the opposite side, from which the fractional length of the path through the channel occupied by the vapor phase can be determined. The chordal void fraction is defined as

$$\varepsilon_{chordal} = \frac{L_G}{L_G + L_L} \qquad [17.1.2]$$

where L_G is the length of the line through the vapor phase and L_L is the length through the liquid phase.

The *cross-sectional* void fraction ε_{c-s} is typically measured using either an optical means or by an indirect approach, such the electrical capacitance of a conducting liquid phase. The cross-sectional void fraction is defined as

$$\varepsilon_{c-s} = \frac{A_G}{A_G + A_L} \qquad [17.1.3]$$

where A_G is the area of the cross-section of the channel occupied by the vapor phase and A_L is that of the liquid phase.

The *volumetric* void fraction ε_{vol} is typically measured using a pair of quick-closing values installed along a channel to trap the two-phase fluid, whose respective vapor and liquid volumes are then determined. The volumetric void fraction is defined as

$$\varepsilon_{vol} = \frac{V_G}{V_G + V_L} \qquad [17.1.4]$$

where V_G is the volume of the channel occupied by the vapor phase and V_L is that of the liquid phase.

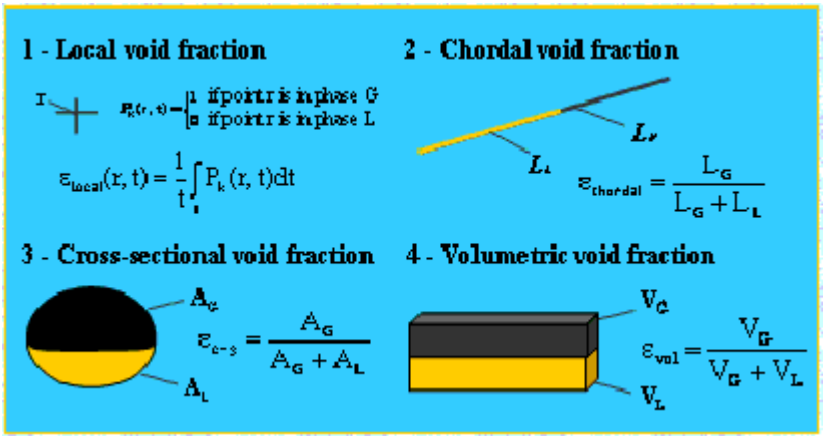

Figure 17.1. Geometrical definitions of void fraction: local (upper left), chordal (upper right), cross-sectional (lower left) and volumetric (lower right).

For those new to the idea of a void fraction of a two-phase flow, it is important to distinguish the difference between void fraction of the vapor phase and the thermodynamic vapor quality x…they do not mean the same thing. To illustrate the difference, consider a closed bottle half full of liquid and the remaining volume occupied by its vapor. The vapor quality is the ratio of the mass of vapor in the bottle to the total mass of liquid plus vapor. If the density ratio of liquid to vapor is 5/1, then the vapor quality is 1/6. Instead, the volumetric void fraction is obtained by applying [17.1.4] and in this case would be equal to 1/2.

The most widely utilized void fraction definition is the cross-sectional average void fraction, which is based on the relative cross-sectional areas occupied by the respective phases. In this chapter, the cross-sectional void fraction of the gas or vapor phase $\varepsilon_{c\text{-}s}$ will henceforth be referred to simply as ε. Cross-sectional void fractions are usually predicted by one of the following types of methods:

- Homogeneous model (which assumes the two phases travel at the same velocity);
- One-dimensional models (which account for differing velocities of the two phases);
- Models incorporating the radial distributions of the local void fraction and flow velocity;
- Models based on the physics of specific flow regimes;
- Empirical and semi-empirical methods.

The principal methods for predicting void fraction are presented in the following sections.

Example 17.1: After applying an optical measurement technique to a two-phase flow, an experimental research group reported the following results:

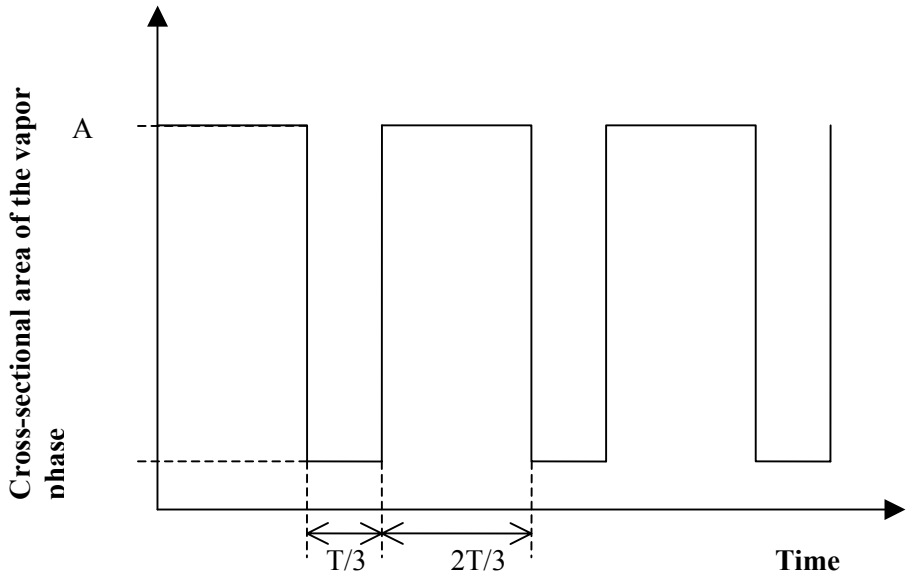

The graph presents the temporal variation of the cross-sectional area of the vapor phase at a fixed axial location along the channel. For a flow having a cross-section of area A, evaluate the local time-averaged void fraction knowing that the period of the signal is T. Assuming the flow to be homogeneous, deduce the corresponding vapor quality (fluid R-134a at 4°C: $\rho_L = 1281$ kg/m^3, $\rho_G = 16.56$ kg/m^3).

Solution: The local time-averaged vapor quality is given by the integral over one time period of the instantaneous void fraction, that is:

$$\varepsilon_{c-s} = \frac{1}{T}\int_{t}^{t+T} \frac{A_G(t)}{A}\,dt$$

In view of the discrete nature of the signal, the integral is equivalent to the following summation:

$$\varepsilon_{c-s} = \frac{1}{TA}\left(\frac{A}{7}\frac{T}{3} + A\frac{2T}{3}\right) = \frac{15}{21} = 0.714$$

With a simple manipulation of the void fraction equation for homogeneous flow (eq. [17.2.4] from the next section), the corresponding vapor quality is given by:

$$x = \frac{\dfrac{\rho_G}{\rho_L}\varepsilon_{c-s}}{\left[\left(\dfrac{\rho_G}{\rho_L} - 1\right)\varepsilon_{c-s} + 1\right]} = 0.031$$

Thus, for a void fraction of about 71%, the corresponding vapor quality is only around 3%. Hence, this is an important fact to keep in mind…vapor void fractions at low vapor qualities are much larger than the

value of the vapor quality itself because of the large difference in the densities of the respective phases (and hence the specific volumes of the two phases).

17.2 Homogeneous Model and Velocity Ratio

17.2.1 Homogeneous Void Fraction

From the definition of the cross-section void fraction of a channel of area A, the mean vapor and liquid velocities are given in terms of the vapor quality x as follows:

$$u_G = \frac{\dot{Q}_G}{A\varepsilon} = \frac{\dot{m}}{\rho_G}\left(\frac{x}{\varepsilon}\right) \qquad [17.2.1]$$

$$u_L = \frac{\dot{Q}_L}{A(1-\varepsilon)} = \frac{\dot{m}}{\rho_L}\left(\frac{1-x}{1-\varepsilon}\right) \qquad [17.2.2]$$

as a function of the volumetric flow rates of the vapor and liquid flows, $\dot{Q}_G$ and $\dot{Q}_L$, respectively. The basis of the homogeneous model is that it assumes that the liquid and vapor phases travel at the same velocities. Thus, equating the above expressions for equal velocities in each phase, one obtains

$$\varepsilon = \frac{\dfrac{x}{\rho_G}}{\left(\dfrac{1-x}{\rho_L}\right)+\left(\dfrac{x}{\rho_G}\right)} \qquad [17.2.3]$$

Rearranging, the homogeneous void fraction, denoted as ε_H, is obtained to be

$$\varepsilon_H = \frac{1}{1+\left(\dfrac{1-x}{x}\right)\dfrac{\rho_G}{\rho_L}} \qquad [17.2.4]$$

The homogeneous void fraction model is reasonably accurate for only a limited range of circumstances. The best agreement is for bubbly and dispersed droplet or mist flows, where the entrained phase travels at nearly the same velocity as the continuous phase. The homogeneous void fraction is also the limiting case as the pressure tends towards the critical pressure, where the difference in the phase densities disappears. Its use is also valid at very large mass velocities and at high vapor qualities.

17.2.2 Definition of the Velocity Ratio

The *velocity ratio* is a concept utilized in separated flow types of models, where it is assumed that the two phases travel at two different mean velocities, u_G and u_L. Note, however, that the velocity ratio is often referred to as the *slip ratio*, although physically there *cannot* be a discontinuity in the two velocities at the interface since a boundary layer is formed in both phases on either side of the interface. Hence, the velocity ratio is only a simplified means for describing relative mean velocities of the two co-existent phases. Introducing this idea into the homogeneous void fraction equation above results in

$$\varepsilon = \frac{1}{1 + \left(\frac{1-x}{x}\right)\frac{\rho_G}{\rho_L} S} \qquad [17.2.5]$$

where the velocity ratio S is

$$S = \frac{u_G}{u_L} \qquad [17.2.6]$$

For equal velocities, this expression reverts to the homogeneous model expression, i.e. S=1. For upward and horizontal co-current flows, u_G is nearly always greater than u_L such that $S \geq 1$. In this case, the homogeneous void fraction ε_H is the upper limit on possible values of ε. For vertical down flows, u_G may be smaller than u_L due to gravity effects such that $S < 1$, in which case the homogeneous void fraction ε_H is the lower limit on the value of ε. Numerous analytical models and empirical correlations have been proposed for determining S, and with this then the void fraction ε. Several approaches are presented in the next sections.

Utilizing the definition of the velocity ratio and the respective definitions above, a relationship between the cross-sectional void fraction and the volumetric void fraction (the latter obtained by the quick-closing valve measurement technique) can be derived, returning to the nomenclature used in Section 17.1:

$$\varepsilon_{vol} = \frac{\varepsilon_{c-s}}{\frac{1}{S}(1-\varepsilon_{c-s}) + \varepsilon_{c-s}} \qquad [17.2.7]$$

Thus, it can be seen that ε_{vol} is only equal to ε_{c-s} for the special case of homogeneous flow and in all other cases the velocity ratio must be known in order to convert volumetric void fractions to cross-sectional void fractions.

17.3 Analytical Void Fraction Models

Various approaches have been utilized to attempt to predict void fractions by analytical means. Typically some quantity, such as momentum or kinetic energy of the two phases, is minimized with the implicit assumption that the flow will tend towards the minimum of this quantity.

17.3.1 Momentum Flux Model

The momentum flux of a fluid is given by

$$\text{momentum flux} = \dot{m}^2 v_H \qquad [17.3.1]$$

where the specific volume of a homogeneous fluid with two phases v_H is

$$v_H = v_G x + v_L(1-x) \qquad [17.3.2]$$

For separated flows, the momentum flux is instead

$$\text{momentum flux} = \dot{m}^2\left[\frac{x^2 v_G}{\varepsilon} + \frac{(1-x)^2 v_L}{1-\varepsilon}\right] \qquad [17.3.3]$$

If the value of the void fraction is assumed to be that obtained when minimizing the momentum flux, the above expression can be differentiated with respect to ε and the derivative of the momentum flux set equal to zero. Comparing the resulting expression to [17.2.5], the velocity ratio for this simple model is

$$S = \left(\frac{\rho_L}{\rho_G}\right)^{1/2} \qquad [17.3.4]$$

17.3.2 Zivi Kinetic Energy Models for Annular Flow

The first Zivi (1964) void fraction model was proposed for annular flow, assuming that no liquid is entrained in the central vapor core. The model is based on the premise that the total kinetic energy of the two phases will seek to be a minimum. The kinetic energy of each phase KE_k is given by

$$KE_k = \frac{1}{2}\rho_k u_k^2 \dot{Q}_k \qquad [17.3.5]$$

where $\dot{Q}_k$ is the volumetric flow rate in m^3/s and u_k is the mean velocity in each phase *k* in m/s. The volumetric flow rate for each phase as

$$\dot{Q}_G = \frac{\dot{m}xA}{\rho_G} \qquad [17.3.6]$$

$$\dot{Q}_L = \frac{\dot{m}(1-x)A}{\rho_L} \qquad [17.3.7]$$

then the corresponding definitions for the velocities of each phase are [17.2.1] and [17.2.2] where the total cross-sectional area of the channel is A. The total kinetic energy of the flow KE is then

$$KE = \sum_{k=1}^{2} KE_k = KE_G + KE_L = \frac{1}{2}\rho_G \frac{\dot{m}^2 x^2}{\varepsilon^2 \rho_G^2}\frac{\dot{m}xA}{\rho_G} + \frac{1}{2}\rho_L \frac{\dot{m}^2(1-x)^2}{(1-\varepsilon)^2\rho_L^2}\frac{\dot{m}(1-x)A}{\rho_L} \qquad [17.3.8]$$

or

$$KE = \frac{A\dot{m}^3}{2}\left[\frac{x^3}{\varepsilon^2\rho_G^2} + \frac{(1-x)^3}{(1-\varepsilon)^2\rho_L^2}\right] = \frac{A\dot{m}^3}{2}y \qquad [17.3.9]$$

where the parameter y is

$$y = \frac{x^3}{\varepsilon^2 \rho_G^2} + \frac{(1-x)^3}{(1-\varepsilon)^2 \rho_L^2} \qquad [17.3.10]$$

Differentiating parameter y with respect to ε in the above expression to find the minimum kinetic energy flow gives

$$\frac{dy}{d\varepsilon} = \frac{-2x^3}{\varepsilon^3 \rho_G^2} + \frac{2(1-x)^3}{(1-\varepsilon)^3 \rho_L^2} = 0 \qquad [17.3.11]$$

The minimum is then found when

$$\frac{\varepsilon}{1-\varepsilon} = \frac{x}{1-x}\left(\frac{\rho_L}{\rho_G}\right)^{2/3} \qquad [17.3.12]$$

Comparing [17.3.12] to [17.2.5], the velocity ratio S is seen by inspection to be

$$S = \frac{u_G}{u_L} = \left(\frac{\rho_L}{\rho_G}\right)^{1/3} \qquad [17.3.13]$$

The velocity ratio for these conditions is therefore only dependent on the density ratio and the Zivi void fraction expression is

$$\varepsilon = \frac{1}{1 + \frac{1-x}{x}\left(\frac{\rho_G}{\rho_L}\right)^{2/3}} \qquad [17.3.14]$$

Zivi also derived a void fraction model for annular flow accounting for liquid entrainment in the vapor core, where the fraction of the liquid entrained as droplets is e. The fraction e is equal to the mass flow rate of droplets divided by the total liquid mass flow rate. Beginning with a summation of the kinetic energies of the vapor, the liquid in the annular film, and the liquid entrained in the vapor (assuming the droplets travel at the same velocity as the vapor, his second void fraction expression is

$$\varepsilon = \frac{1}{1 + e\left(\frac{1-x}{x}\right)\left(\frac{\rho_G}{\rho_L}\right) + (1-e)\left(\frac{1-x}{x}\right)\left(\frac{\rho_G}{\rho_L}\right)^{2/3}\left[\frac{1 + e\left(\frac{1-x}{x}\right)\left(\frac{\rho_G}{\rho_L}\right)}{1 + e\left(\frac{1-x}{x}\right)}\right]^{1/3}} \qquad [17.3.15]$$

The actual value of e is unknown and Zivi does not present a method for its prediction. However, the limits on feasible values of e are as follows:

- For e = 0, the above expression reduces to the prior expression of Zivi for the void fraction, namely [17.3.14];

- For e = 1, the above expression reduces to the homogeneous void fraction equation.

Figure 17.2 illustrates the influence of the entrained liquid fraction e on void fraction for ammonia at a saturation temperature of 4°C. The effect is the most evident at low qualities where the value of the void fraction changes significantly with the entrained liquid fraction e.

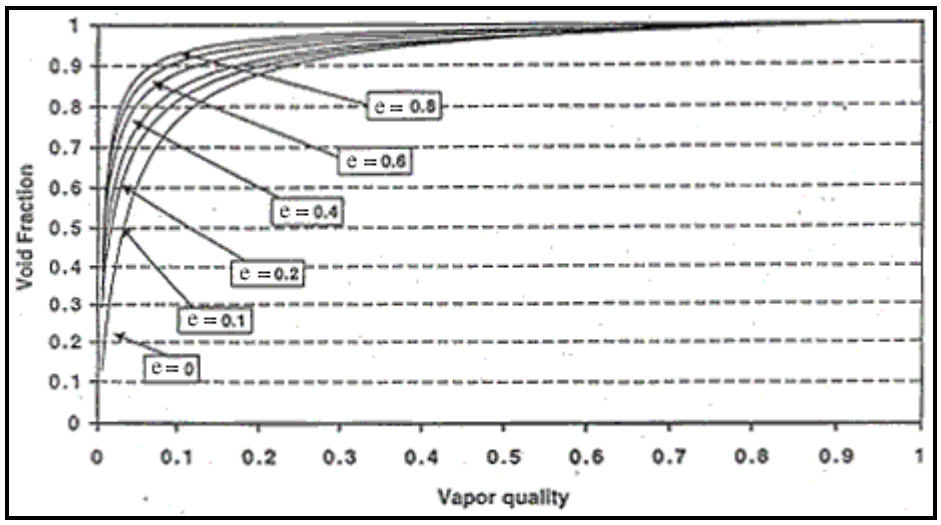

Figure 17.2. Influence of entrained liquid on void fraction for ammonia using Zivi (1964) equation [figure taken from Zürcher (2000)].

Example 17.2: Determine the void fraction for the following vapor qualities (0.01, 0.05, 0.1, 0.25, 0.50, 0.75, 0.95) using the following methods: homogeneous flow, momentum flux model and both of Zivi's expressions. The liquid density is 1200 kg/m^3 and the gas density is 20 kg/m^3. Assume the liquid entrainment is equal to 0.4.

Solution: The density ratio of ρ_G/ρ_L is equal to 0.0167.

Quality, x	0.01	0.05	0.10	0.25	0.50	0.75	0.95
(1-x)/x	99	19	9	3	1	0.3333	0.0526
$\varepsilon=\varepsilon_H$ Homogeneous [17.2.4]	0.377	0.759	0.870	0.952	0.984	0.994	0.999
ε [17.3.4] Momentum flux	0.0726	0.290	0.463	0.721	0.886	0.959	0.993
ε [17.3.14] Zivi #1	0.134	0.446	0.630	0.836	0.939	0.979	0.997
ε [17.3.15] Zivi #2	0.251	0.665	0.784	0.900	0.960	0.985	0.998

Hence, at low vapor qualities there is a wide range in the values of the void fraction while at high vapor qualities the range is relatively small.

17.3.3 Levy Momentum Model

Levy (1967) derived a momentum void fraction model with forced convective flow boiling of water in mind. Starting with the momentum equation, he assumed that the sums of the frictional and static head losses in each phase are equal. He also assumed that momentum is exchanged between the phases constantly as x, ε or ρ_G/ρ_L vary, such that the flow tends to maintain an equality of sum of the frictional

and static head losses in each phase. His analysis reduces to the following implicit expression for the void fraction:

$$x = \frac{\varepsilon(1-2\varepsilon) + \varepsilon\sqrt{(1-2\varepsilon)^2 + \varepsilon\left[2\frac{\rho_L}{\rho_G}(1-\varepsilon)^2 + \varepsilon(1-2\varepsilon)\right]}}{2\frac{\rho_L}{\rho_G}(1-\varepsilon)^2 + \varepsilon(1-2\varepsilon)} \qquad [17.3.16]$$

Levy found that there was good agreement between his void fraction model and experimental data only at high pressures.

17.4 Empirical Void Fraction Equations

17.4.1 Smith Separated Flow Model

Similar to Levy (1960), Smith (1969) assumed a separated flow consisting of a liquid phase and a gas phase with a fraction e of the liquid entrained in the gas as droplets. He also assumed that the momentum fluxes in the two phases were equal. On this basis, he arrived at the following velocity ratio expression:

$$S = e + (1-e)\left[\frac{\left(\frac{\rho_L}{\rho_G}\right) + e\left[\frac{1-x}{x}\right]}{1 + e\left[\frac{1-x}{x}\right]}\right]^{1/2} \qquad [17.4.1]$$

This expression simplifies to [17.2.4] when e = 1 and to [17.3.4] when e = 0 at its extremes as should be expected. His entrainment fraction e was set empirically to a value of 0.4 by comparing the above expression to three independent sets of void fraction data measured by three different techniques. He thus claimed that the method was valid for all conditions of two-phase flow irrespective of pressure, mass velocity, flow regime and enthalpy change, predicting most of the data to within ±10%. Setting e equal to 0.4, the above expression reduces to the following simple relationship for void fraction:

$$\varepsilon = \frac{1}{1 + 0.79\left(\frac{1-x}{x}\right)^{0.78}\left(\frac{\rho_G}{\rho_L}\right)^{0.58}} \qquad [17.4.2]$$

Figure 17.3 depicts the influence of the entrained liquid fraction e on void fraction in the Smith method for ammonia at a saturation temperature of 4°C. The entrained liquid effect is the stronger here than in the Zivi method shown in Figure 17.2.

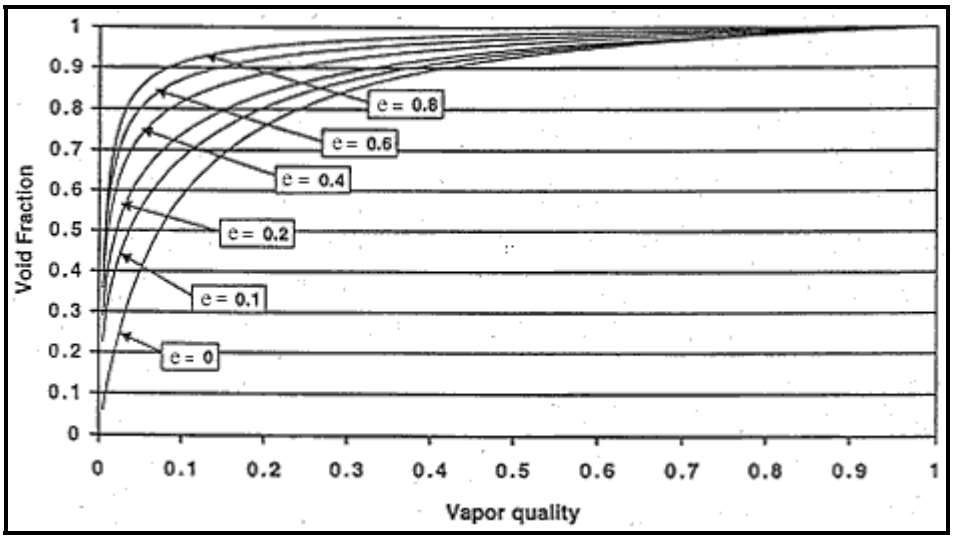

Figure 17.3. Influence of entrained liquid on void fraction by Smith (1969) equation with ammonia [figure taken from Zürcher (2000)].

17.4.2 Chisholm Method

Chisholm (1972) arrived at the following correlation for the velocity ratio

$$S = \frac{u_G}{u_L} = \left(\frac{\rho_L}{\rho_H}\right)^{1/2} = \left[1 - x\left(1 - \frac{\rho_L}{\rho_G}\right)\right]^{1/2} \qquad [17.4.3]$$

This expression results from simple annular flow theory and application of the homogeneous theory to define the homogenous fluid density ρ_H, producing approximately equal frictional pressure gradients in each phase. It gives values of ε similar to those predicted by Smith (1969), except at high vapor qualities. The Chisholm correlation is also notable because it goes to the correct thermodynamic limits. Thus, $S \rightarrow 1$ as $x \rightarrow 0$, i.e. at very low void fraction the velocity of the very small bubbles should tend towards the liquid velocity since their buoyancy will be negligible. Also, $S \rightarrow (\rho_L/\rho_G)^{1/2}$ as $x \rightarrow 1$. The latter limit happens to correspond to when the momentum flow is a minimum, i.e. expression [17.3.4]. Many empirical methods do not go to these correct limits when $x \rightarrow 0$ and/or $x \rightarrow 1$.

Example 17.3: For the same conditions as in Example 17.2, determine the void fraction for the following vapor qualities (0.01, 0.05, 0.1, 0.25, 0.50, 0.75, 0.95) using the methods of Smith and Chisholm. Assume the liquid entrainment is equal to 0.4. Also, determine the velocity ratio using the Chisholm equation.

Solution: The density ratio of ρ_G/ρ_L is equal to 0.0167.

Quality, x	0.01	0.05	0.10	0.25	0.50	0.75	0.95
ε [17.4.2] Smith	0.274	0.578	0.710	0.852	0.932	0.970	0.993
S [17.4.3]	1.26	1.99	2.63	3.97	5.52	6.73	7.55
ε (Chisholm)	0.325	0.614	0.717	0.834	0.916	0.964	0.993

Hence, these two methods give similar results for the void fraction for this density ratio, except at the lowest quality. The velocity ratio is seen to increase from a modest value of 1.26 up to 7.55.

17.4.3 Drift Flux Model

The drift flux model was developed principally by Zuber and Findlay (1965), although Wallis (1969) and Ishii (1977) in particular and others have added to its development. Its original derivation was presented in Zuber and Findlay (1965) and a comprehensive treatment of the basic theory supporting the drift flux model can be found in Wallis (1969). Below, methods for determining void fraction based on the drift flux model are presented first for vertical channels and then a method is given for horizontal tubes. Also, the general approach to include the effects of radial void fraction and velocity profiles within the drift flux model is presented.

The drift flux U_{GL} represents the volumetric rate at which vapor is passing forwards or backwards through a unit plane normal to the channel axis that is itself traveling with the flow at a velocity U where $U = U_G + U_L$ and thus U remains a local parameter, where superficial velocity of the vapor U_G and the superficial velocity of the liquid U_L are defined as:

$$U_G = u_G \varepsilon \qquad [17.4.4a]$$

and

$$U_L = u_L (1 - \varepsilon) \qquad [17.4.4b]$$

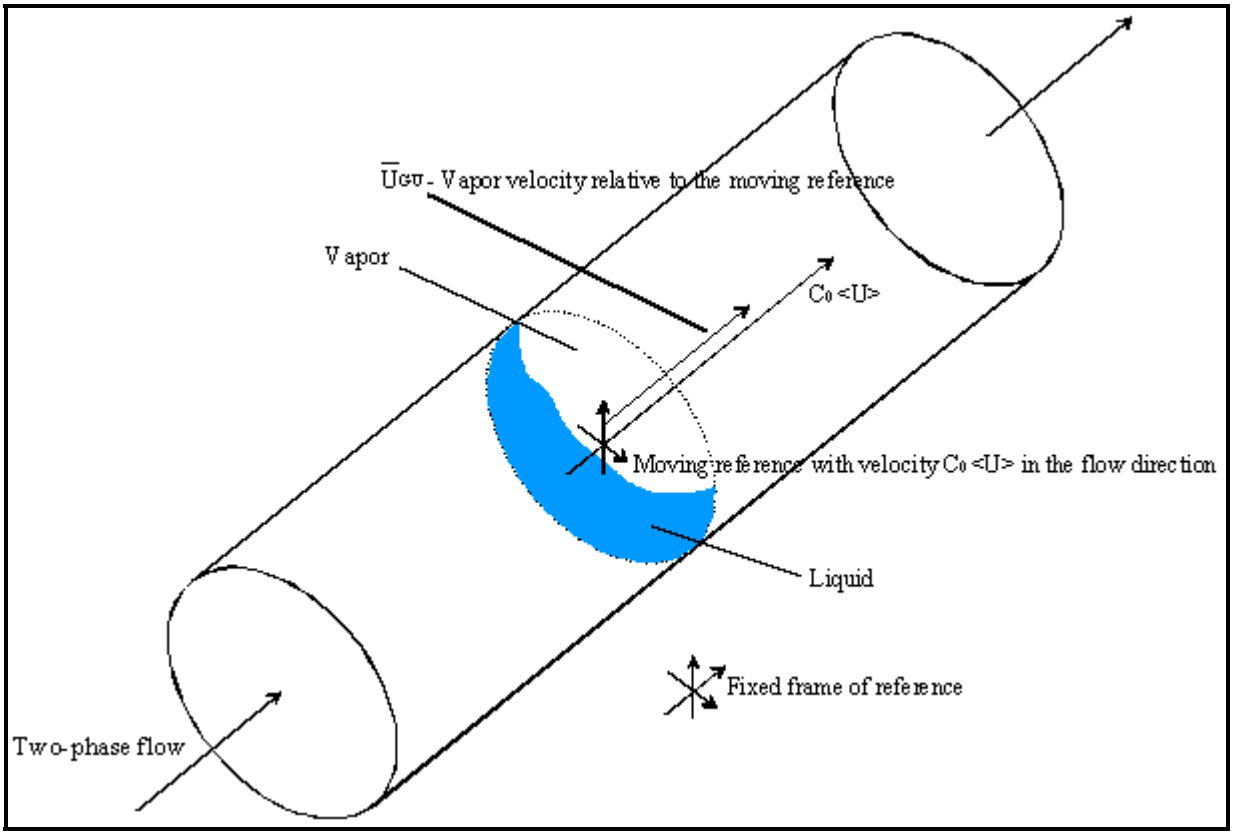

Figure 17.4. Drift flux model.

Here, u_G and u_L refer to the actual local velocities of the vapor and liquid and ε is the local void fraction, as defined by [17.1.1] but dropping the subscript *local* here. The physical significance of the drift velocity is illustrated in Figure 17.4. These expressions are true for one-dimension flow or at any local point in the flow. Based on these three quantities, the drift velocities can now be defined as $U_{GU} = u_G - U$ and $U_{LU} =$

$u_L - U$. Now proceeding as a one-dimensional flow and taking these parameters as local values in their respective profiles across the channel and denoting the cross-sectional average properties of the flow with < >, which represents the average of a quantity F over the cross-sectional area of the duct as $\langle F \rangle = (\int_A F dA)/A$. The mean velocity of the vapor $\langle u_G \rangle$ is thus given by the above expressions to be $\langle u_G \rangle = \langle U \rangle + \langle U_{GU} \rangle = \langle U_G/\varepsilon \rangle$. In addition, $\langle U_G \rangle = \langle u_G \varepsilon \rangle$ and also

$$< U_G > = \frac{\dot{Q}_G}{A} \qquad [17.4.5a]$$

and

$$< U_L > = \frac{\dot{Q}_L}{A} \qquad [17.4.5b]$$

The weighed mean velocity $\bar{u}_G$ is instead given by $\bar{u}_G = \langle u_G \varepsilon \rangle / \langle \varepsilon \rangle$. The definition of the drift velocity of the vapor phase U_{GU} yields the following expression for $\bar{u}_G$:

$$\bar{u}_G = \frac{< U_G >}{< \varepsilon >} = \frac{< \varepsilon U >}{< \varepsilon >} + \frac{< \varepsilon U_{GU} >}{< \varepsilon >} \qquad [17.4.6]$$

where $\langle \varepsilon \rangle$ is the cross-sectional average of the local void fraction. The drift flux is the product of the local void fraction with the local drift velocity

$$U_{GL} = \varepsilon U_{GU} \qquad [17.4.7a]$$

Using the fact that $U_{GU} = u_G - U$ combined with the expression for u_G in [17.4.4a], rearranging and substituting for U_{GU} in [17.4.7a], the drift flux U_{GL} is also given by the expression:

$$U_{GL} = (1 - \varepsilon) U_G - \varepsilon U_L \qquad [17.4.7b]$$

A distribution parameter C_o can now defined as

$$C_o = \frac{< \varepsilon U >}{< \varepsilon >< U >} \qquad [17.4.7c]$$

This ratio accounts for the mathematical difference in averaging ε and U as a product rather than separately. A weighed mean drift velocity $\bar{U}_{GU}$ can also be defined as

$$\bar{U}_{GU} = \frac{< U_{GL} >}{< \varepsilon >} \qquad [17.4.7d]$$

Then the following expression is obtained

$$\bar{u}_G = \frac{< U_G >}{< \varepsilon >} = C_o < U > + \bar{U}_{GU} \qquad [17.4.8]$$

Now dividing through by $\langle U \rangle$ gives

$$\frac{\bar{u}_G}{<U>} = \frac{<\beta>}{<\varepsilon>} = C_o + \frac{\bar{U}_{GU}}{<U>} \qquad [17.4.9]$$

or

$$<\varepsilon> = \frac{<\beta>}{C_o + \dfrac{\bar{U}_{GU}}{<U>}} \qquad [17.4.10]$$

where <β> is the volumetric quality defined as

$$<\beta> = \frac{<U_G>}{<U>} = \frac{<U_G>}{<U_G> + <U_L>} = \frac{\dot{Q}_G}{\dot{Q}_G + \dot{Q}_L} \qquad [17.4.11]$$

where the volumetric flow rates of each phase are obtainable from [17.3.6] and [17.3.7]. For the case where there is no relative motion between the two phases, that is when $\bar{U}_{GU} = 0$, then

$$<\varepsilon> = \frac{<\beta>}{C_o} \qquad [17.4.12]$$

Thus, it is evident that C_o is an empirical factor that corrects one-dimensional homogeneous flow theory to separated flows to account for the fact that the void concentration and velocity profiles across the channel can vary independently of one another. It follows then for homogeneous flow that

$$<\varepsilon> = <\beta> \qquad [17.4.13]$$

The above expression [17.4.11] demonstrates that <β> is the ratio of the volumetric vapor (or gas) flow rate to the total volumetric flow rate. Rearranging that expression in terms of the specific volumes of the two phases, v_G and v_L, gives:

$$<\beta> = \frac{x v_G}{x v_G + (1-x) v_L} \qquad [17.4.14a]$$

The two-phase density ρ can be expressed as the inverse of the two-phase specific volume v as:

$$v = x v_G + (1-x) v_L \quad \Rightarrow \quad \rho = \frac{1}{v} = \frac{1}{\dfrac{x}{\rho_G} + \dfrac{1-x}{\rho_L}} \qquad [17.4.14b]$$

Furthermore, the mass velocity can be written as follows:

$$\dot{m} = \rho <U> \qquad [17.4.14c]$$

Now, using these three expressions, [17.4.10] for <ε> can be rewritten as:

$$<\varepsilon> = \frac{\dfrac{x}{\rho_G}}{\dfrac{x}{\rho_G}+\dfrac{1-x}{\rho_L}}\left[C_o + \frac{\overline{U}_{GU}}{\dot{m}\left(\dfrac{x}{\rho_G}+\dfrac{1-x}{\rho_L}\right)}\right]^{-1} \qquad [17.4.14d]$$

Rearranging, the simplified form of the general drift flux void fraction equation is

$$<\varepsilon> = \frac{x}{\rho_G}\left[C_o\left(\frac{x}{\rho_G}+\frac{1-x}{\rho_L}\right)+\frac{\overline{U}_{GU}}{\dot{m}}\right]^{-1} \qquad [17.4.14e]$$

The above expression shows that void fraction is a function of mass velocity, while the previously presented analytical theories did not capture this effect. **Further note that elsewhere in this book, i.e. other than here in Section 17.4 on drift flux models, the cross-sectional average of the local void fraction <ε> is written simply as ε**.

The drift flux model can be used with or without reference to the particular flow regime as shown by Ishii (1977). The drift flux model, however, is only valuable when the drift velocity is significantly larger than the total volumetric flux, say when $\bar{U}_{GU}$ is larger than 0.05<U>. Also, note that the above drift flux equation [17.4.14e] reduces to the homogeneous void fraction when $C_o = 1$ and either $\bar{U}_{GU} = 0$ or the mass velocity becomes very large. Several of its applications are discussed below.

At *elevated pressures*, Zuber et al. (1967) have shown that using

$$C_o = 1.13 \qquad [17.4.15]$$

with

$$\overline{U}_{GU} = 1.41\left[\frac{\sigma g(\rho_L-\rho_G)}{\rho_L^2}\right]^{1/4} \qquad [17.4.16]$$

in [17.4.14e] gives a good representation of their data for R-22 and similar data for water-steam, regardless of the flow regime, and includes surface tension into the method.

For the *bubbly flow* regime with one-dimensional vertical upflow of small, isolated bubbles without coalescence, Wallis (1969) has suggested the following equations to use in the drift flux model:

$$C_o = 1.0 \qquad [17.4.17]$$

$$\overline{U}_{GU} = 1.53\left[\frac{\sigma g(\rho_L-\rho_G)}{\rho_L^2}\right]^{1/4} \qquad [17.4.18]$$

It is notable that this expression of $\bar{U}_{GU}$ can be interpreted to represent the buoyancy effect of the bubbles on the vapor rise velocity, increasing the vapor velocity with respect to a homogeneous flow. Also for the *bubbly* vertical upflow regime, Zuber et al. (1967) recommended using [17.4.16] where the value of C_o is

dependent on the reduced pressure p_r and channel internal diameter d_i, depending on channel size and shape as follows:

- For tubes with $d_i > 50$ mm: $C_o = 1 - 0.5p_r$ (except for $p_r < 0.5$ where $C_o = 1.2$);
- For tubes with $d_i < 50$ mm: $C_o = 1.2$ for $p_r < 0.5$;
- For tubes with $d_i < 50$ mm: $C_o = 1.2 - 0.4(p_r - 0.5)$ for $p_r > 0.5$;
- For rectangular channels: $C_o = 1.4 - 0.4p_r$.

For *slug* flows, they recommended using

$$C_o = 1.2 \qquad [17.4.19]$$

$$\overline{U}_{GU} = 0.35\left[\frac{g(\rho_L - \rho_G)d_i}{\rho_L}\right]^{1/2} \qquad [17.4.20]$$

For annular flow, Ishii et al. (1976) proposed using

$$C_o = 1.0 \qquad [17.4.21]$$

$$\overline{U}_{GU} = 23\left(\frac{\mu_L U_L}{\rho_G d_i}\right)\left(\frac{\rho_L - \rho_G}{\rho_L}\right) \qquad [17.4.22]$$

The latter expression introduces the effect of liquid dynamic viscosity on void fraction. Ishii (1977) has also given some additional recommendations. For *vertical downflow*, the sign of $\bar{U}_{GU}$ in [17.4.14e] is changed.

Effect of Non-Uniform Flow Distributions. The definition of C_o given by [17.4.7c] may be rewritten for integration of the void fraction profile and the velocity profile as

$$C_o = \frac{\frac{1}{A}\int_A \varepsilon U dA}{\left[\frac{1}{A}\int_A \varepsilon dA\right]\left[\frac{1}{A}\int_A U dA\right]} \qquad [17.4.23]$$

Its value is thus seen to depend on the distribution of the local void fraction and local phase velocities across the flow channel. As an example, Figures 17.5 and 17.6 depict some experimentally measured values of radial liquid velocity and void fraction profiles for flow of air and water inside a 50 mm bore vertical tube obtained by Malnes (1966). In Figure 17.5, the typical velocity profile for all liquid flow is shown for $<\varepsilon>= 0$ at two different flow rates. For cross-sectional average void fractions from 0.105 to 0.366, the effect of the gas voids on the velocity profile is particularly significant near the wall, giving rise to very high velocity gradients before the velocity levels off in the central portion of the tube. The radial void fraction goes through sharp peaks near the wall as illustrated in Figure 17.6. Hence, the reduction in the local effective viscosity of the flow by the presence of the gas gives rise to the steep velocity gradient.

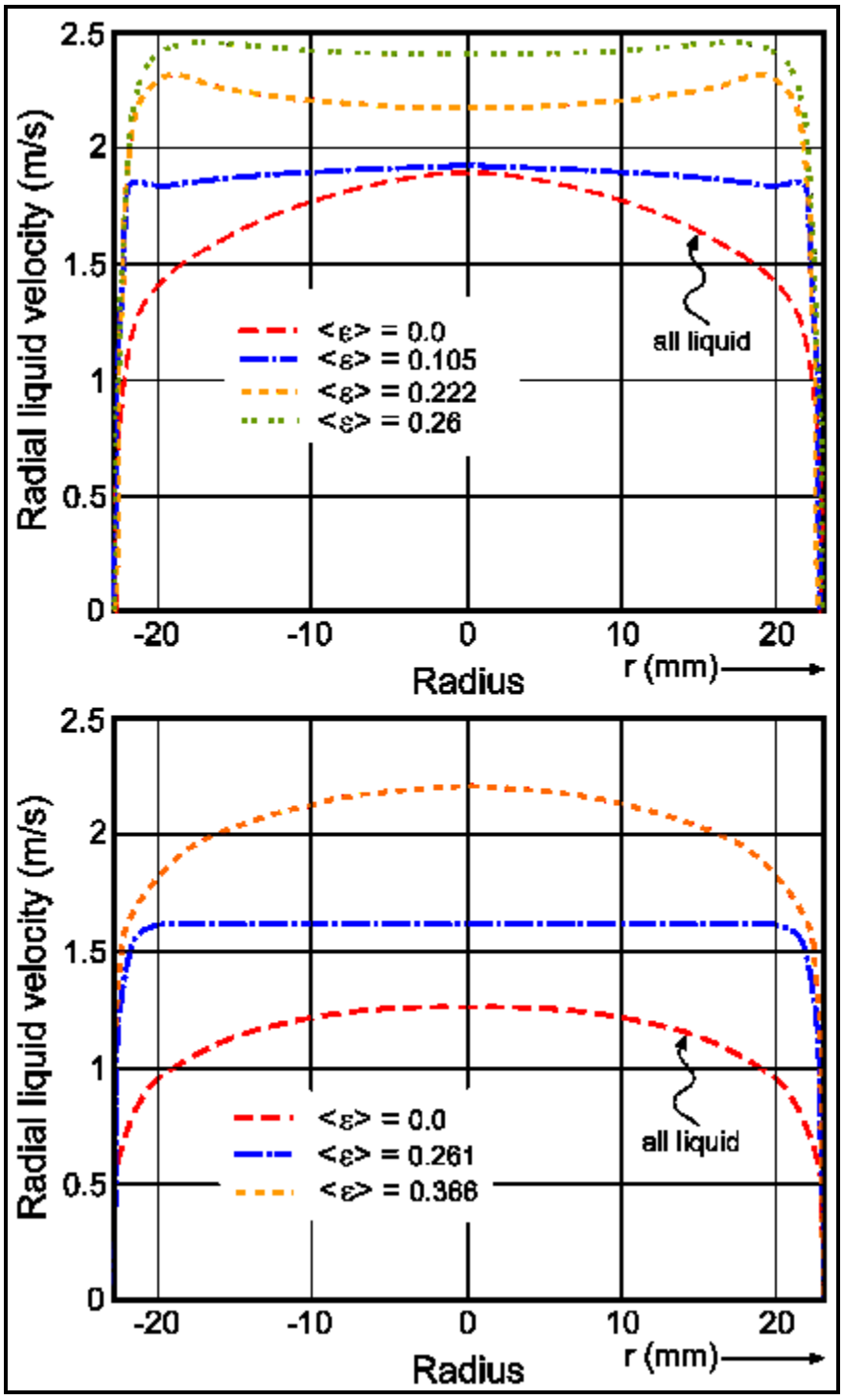

Figure 17.5. Radial liquid velocity profiles for air-water flow measured by Malnes (1966).

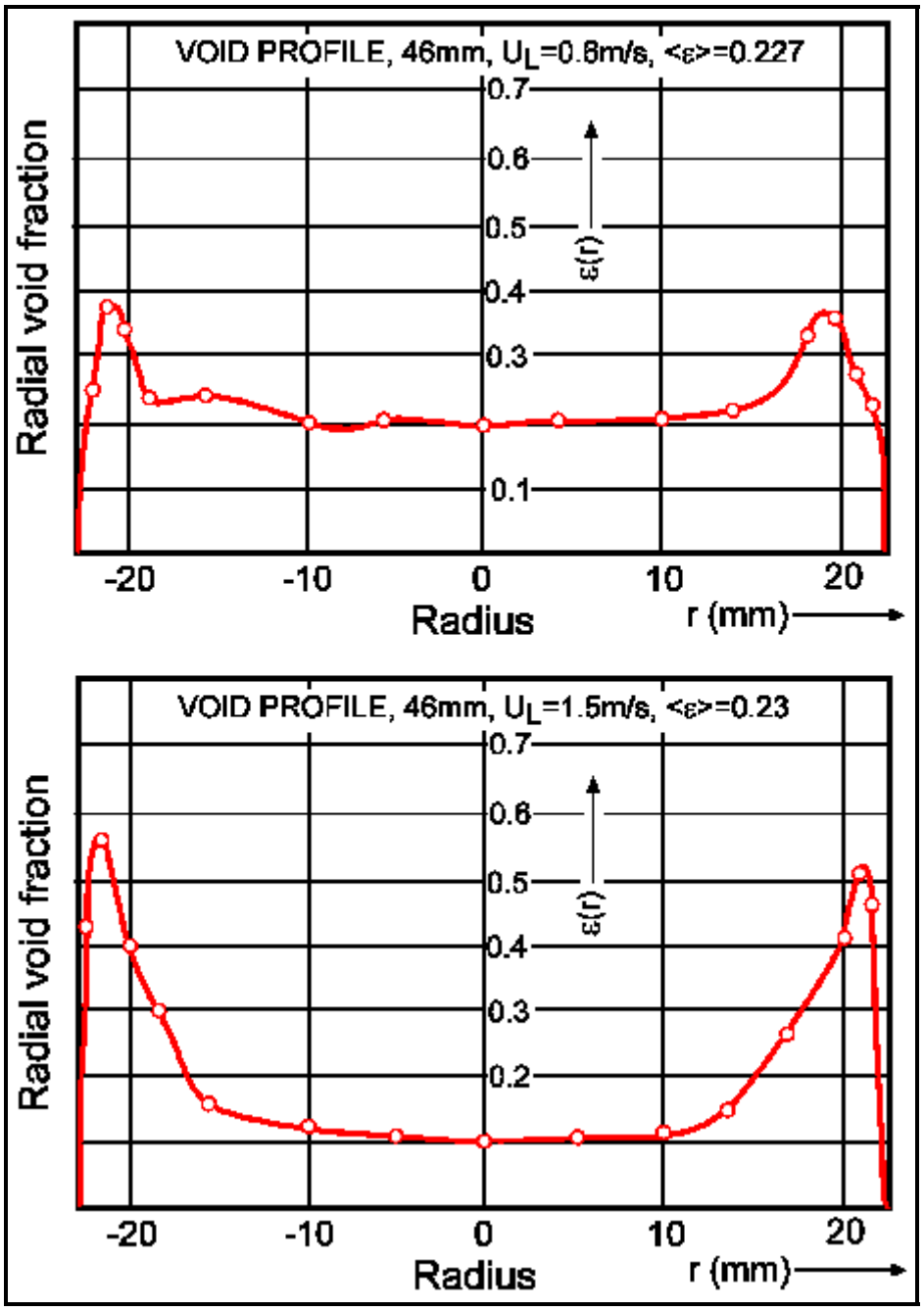

Figure 17.6. Radial void fraction profiles for air-water flow measured by Malnes (1966).

Assuming an axially symmetric flow through a vertical circular pipe of internal radius r_i and assuming that the flow distributions are given by the following radial functions,

$$\frac{U}{U_c} = 1 - \left(\frac{r}{r_i}\right)^m \qquad [17.4.24]$$

$$\frac{\varepsilon - \varepsilon_w}{\varepsilon_c - \varepsilon_w} = 1 - \left(\frac{r}{r_i}\right)^n \qquad [17.4.25]$$

where the subscripts c and w refer to the values at the centerline and the wall, Zuber and Findlay (1965) integrated [17.4.23] to obtain the following expression for the distribution parameter C_o

$$C_o = 1 + \frac{2}{m+n+2}\left[1 - \frac{\varepsilon_w}{<\varepsilon>}\right] \qquad [17.4.26]$$

when expressed in terms of ε_w or

$$C_o = \frac{m+2}{m+n+2}\left[1 + \frac{\varepsilon_c}{<\varepsilon>}\left(\frac{n}{m+2}\right)\right] \qquad [17.4.27]$$

when expressed in terms of ε_c. They noted that if the void fraction is uniform across the channel, i.e. if $\varepsilon_w = \varepsilon_c = <\varepsilon>$, then it follows that $C_o = 1$. If $\varepsilon_c > \varepsilon_w$, then $C_o > 1$. On the other hand, if $\varepsilon_c < \varepsilon_w$, then $C_o < 1$. Furthermore, if m is assumed to be equal to n and the flow is adiabatic ($\varepsilon_w = 0$), then [17.4.26] reduces to

$$C_o = \frac{n+2}{n+1} \qquad [17.4.28]$$

Lahey (1974) presented an interesting picture of the variation in radial void fraction and values of C_o for different types of flow patterns in vertical upflow. His diagram is reproduced in Figure 17.7, illustrating void fraction profiles from an inlet condition of all liquid ($<\varepsilon> = 0$) up to complete evaporation with all vapor ($<\varepsilon> = 1$) with the corresponding change in typical values of C_o. The value of C_o starts out at the inlet for completely subcooled liquid equal to zero. For subcooled bubbly flow, the vapor is formed at the wall and condenses in the subcooled bulk, such that $C_o < 1$. Once saturation conditions are reached at x = 0, the radial void fraction at the center of the tube begins to rise as the bubbles stop condensing and the value of C_o climbs towards 1.0 as bubbly flow becomes more developed. Then, the value becomes greater than 1.0 for slug flows as the radial void fraction at the center of the tube increases as the flow cycles between all vapor when large Taylor bubbles are passing and essentially bubbly flow values as the liquid slugs pass through. It then tends back towards a value of 1.0 in annular flows, where the radial void fraction in the central core approaches 1.0 depending on the level of liquid entrainment and the variation in radial void fraction in the annular film reflects the passage of interfacial waves and the effect of vapor bubbles entrained in the annular liquid film. Finally C_o leaves with a value of unity for 100% vapor.

Rouhani-Axelsson Correlations. Rouhani and Axelsson (1970) correlated the drift velocity for vertical channels as

$$\overline{U}_{GU} = 1.18\left[\frac{g\sigma(\rho_L - \rho_G)}{\rho_L^2}\right]^{1/4} \qquad [17.4.29]$$

where

- $C_o = 1.1$ for mass velocities greater than 200 kg m^{-2} s^{-1};
- $C_o = 1.54$ for mass velocities less than 200 kg m^{-2} s^{-1}.

Instead, the following correlation of Rouhani (1969) can be used for C_o over a wide range of mass velocities:

$$C_o = 1 + 0.2(1-x)\left(\frac{g d_i \rho_L^2}{\dot{m}^2}\right)^{1/4} \qquad [17.4.30]$$

This expression is valid for void fractions larger than 0.1. By combining these expressions with [17.4.14e], it is possible to obtain an explicit value for <ε>.

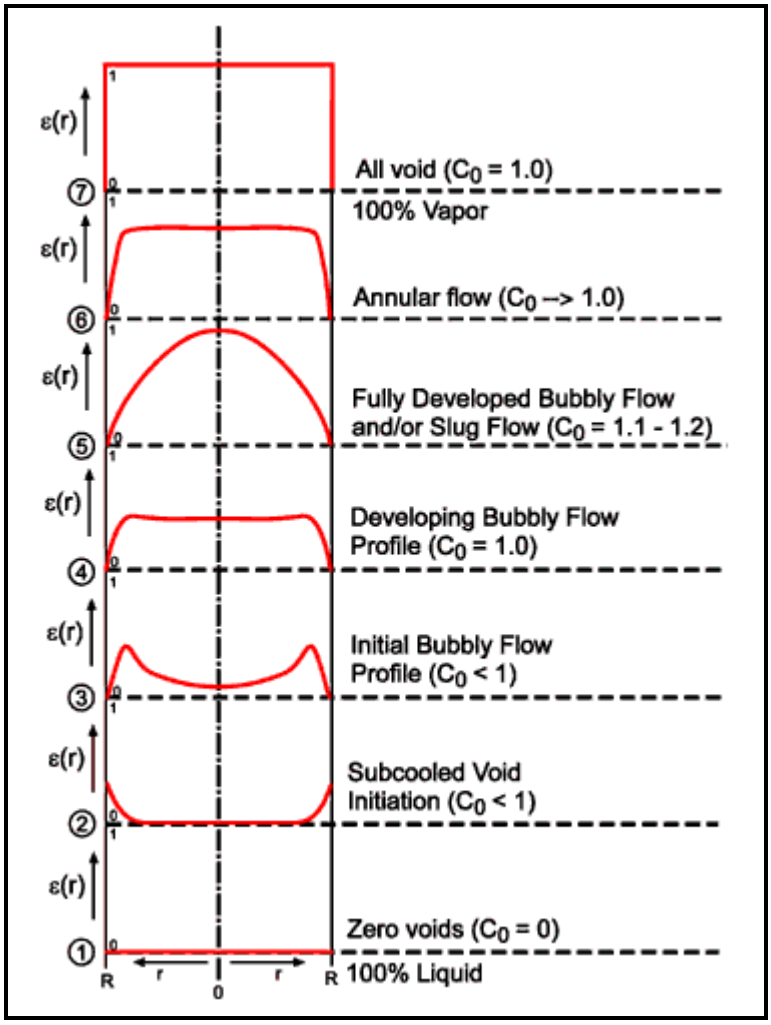

Figure 17.7. Void fraction profiles for selected flow regimes as presented by Lahey (1974).

Horizontal tubes. All the above methods are for ***vertical*** tubes. For ***horizontal*** tubes, Steiner (1993) reports that the following method of Rouhani (1969) is in good agreement with experimental data, whose modified form was chosen in order to go to the correct limit of <ε> = 1 at x = 1:

$$C_o = 1 + c_o(1-x) \qquad [17.4.31]$$

where $c_o = 0.12$ and the term (1-x) has been added to the other expression to give:

$$\overline{U}_{GU} = 1.18(1-x)\left[\frac{g\sigma(\rho_L - \rho_G)}{\rho_L^2}\right]^{1/4} \qquad [17.4.32]$$

Figure 17.8 depicts the influence of mass velocity on void fraction applying [17.4.31] to R-410A at 40°C in an 8 mm tube together with a comparison to the homogeneous void fraction and that predicted using the first method of Zivi above. The effect of mass velocity becomes more evident as mass velocity decreases, shown here for mass velocities of 75, 200 and 500 kg/m^{2}s, while the method of Zivi does not account for this effect. Regarding the best choice of void fraction prediction method to use for horizontal flows, Wojtan, Ursenbacher and Thome (2003) have measured 238 time-averaged cross-sectional void fractions for stratified, stratified-wavy and some slug flows for R-22 and R-410A at 5°C inside an 13.6 mm horizontal glass tube using a new optical measurement technique, processing about 227,000 images. Figure 17.9 shows a comparison of predictions using [17.4.31] and [17.4.32], and the homogeneous model as a reference, to one set of their data for R-410A. In general, this Rouhani drift flux method gave an average deviation of 1.5%, a mean deviation of 7.7% and a standard deviation of 14.8% and was the best of the methods tested.

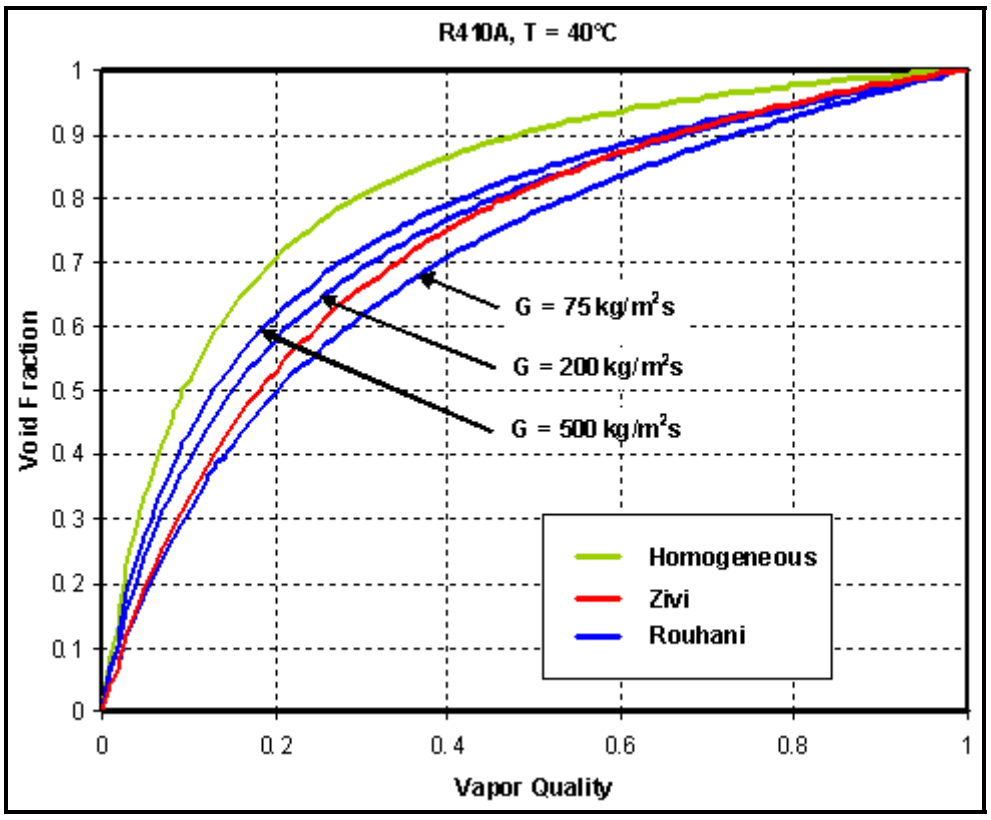

Figure 17.8. Void fractions predicted by various methods for R-410A in an 8 mm tube

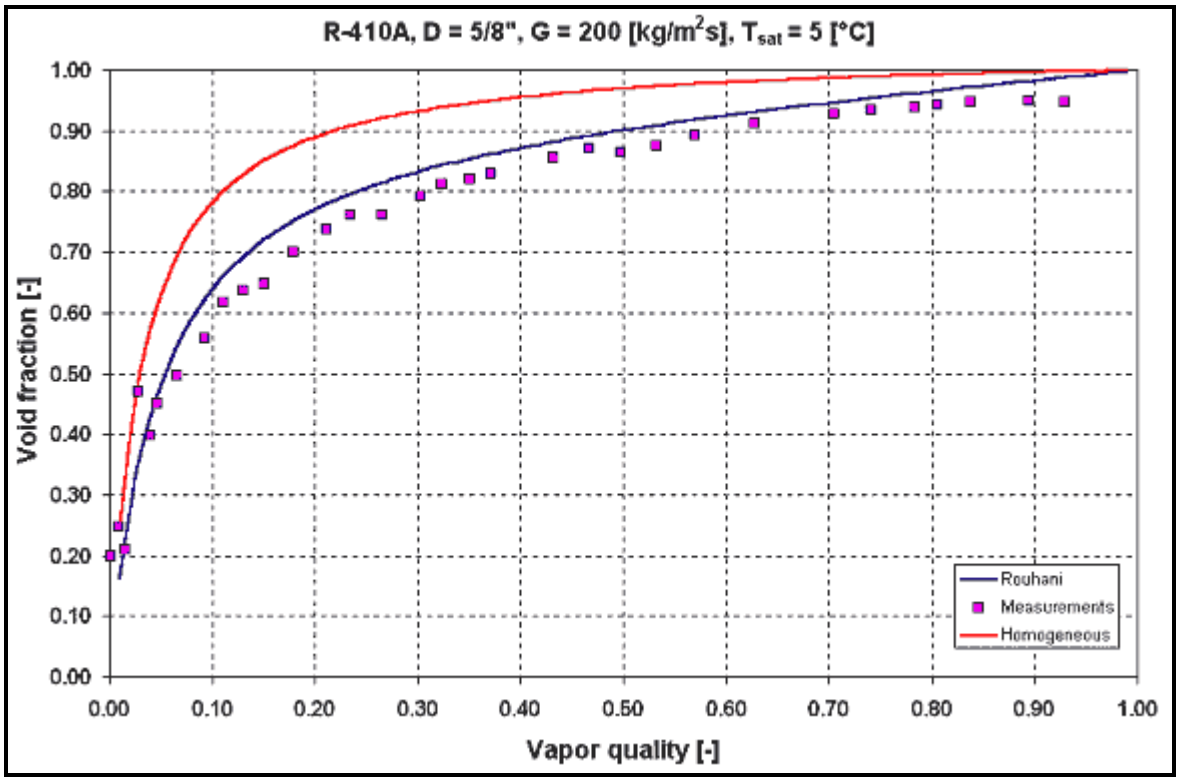

Figure 17.9. Void fractions for R-410A measured by Wojtan, Ursenbacher and Thome (2003).

Example 17.4: Determine the void fractions using expression [17.4.30] for the following qualities (0.1, 0.50, 0.95) for a fluid flowing at a rate of 0.1 kg/s in a vertical tube of 22 mm internal diameter. The fluid has the following physical properties: liquid density is 1200 kg/m^3, gas density is 20 kg/m^3 and surface tension is 0.012 N/m.

Solution: The mass velocity for this situation is 263.1 kg/m^{2}s while the gravitational acceleration g = 9.81 m/s^2. The results of the calculation are shown in the table below.

Quality, x	0.10	0.50	0.95
C_o [17.4.30]	1.262	1.146	1.015
$\bar{U}_{GU}$ [17.4.29]	0.10525	0.05847	0.00585
$\langle\varepsilon\rangle$ [17.4.14e]	0.653	0.852	0.984

The variation of the value of C_o is from 1.262 to 1.015 compared to the fixed value of 1.1 for mass velocities greater than 200 kg/m^{2}s. The void fraction values here can be compared to those in Examples 17.1 and 17.2.

17.5 Comparison of Void Fraction Methods for Tubular Flows

Most expressions for predicting void fraction are actually methods for determining the velocity ratio S. Experimental studies show that the velocity ratio depends on the following parameters in descending order of importance according to Ginoux (1978):

1. Physical properties (in particular as ratios of ρ_G/ρ_L and μ_G/μ_L, respectively);

2. Local quality;
3. Mass velocity;
4. Various secondary variables (tube diameter, inclination and length, heat flux and flow pattern).

Butterworth (1975) has shown that many cross-sectional void fraction equations can be fit to a standard expression form of

$$\varepsilon = \left[1 + n_B \left(\frac{1-x}{x} \right)^{n_1} \left(\frac{\rho_G}{\rho_L} \right)^{n_2} \left(\frac{\mu_L}{\mu_G} \right)^{n_3} \right]^{-1} \qquad [17.5.1]$$

which allows for a comparison to be made and also inconsistencies to be noted. For instance, if the densities and viscosities in both phases are equal, i.e. $\rho_L = \rho_G$ and $\mu_L = \mu_G$, then the void fraction should be equal to the quality x. This means that n_B and n_1 should be equal to 1.0 in all void fraction equations in order to be valid at the limit when the critical pressure is approached. Also notable is the fact that the exponent on the density ratio is always less than that of the homogeneous model. Importantly, some methods include the influence of viscosity while others do not.

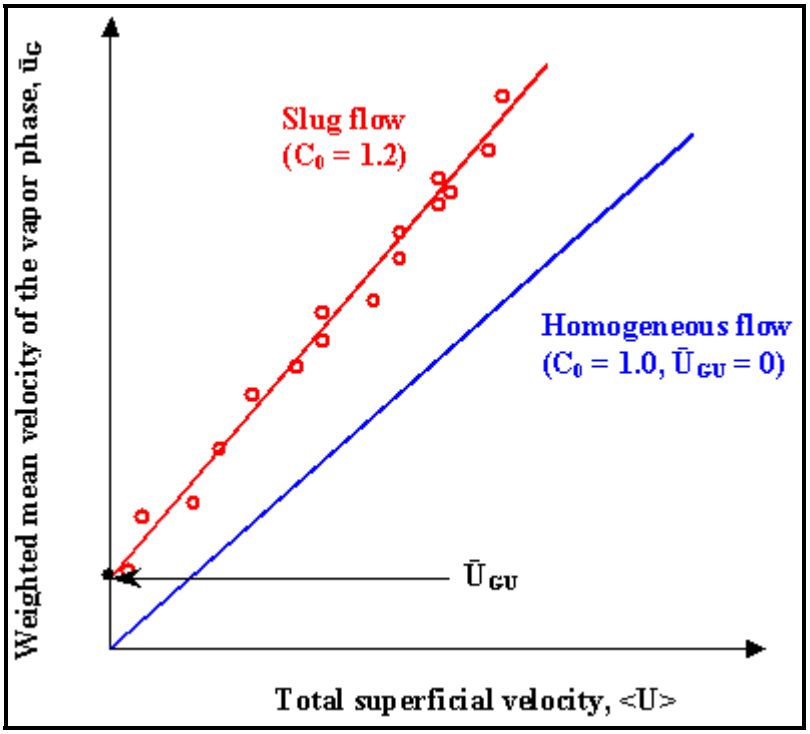

Figure 17.10. Graphical representation of the drift flux model.

There is another important consideration to make with respect to the prediction methods for void fraction…which is the best general approach? The drift flux model appears to be the preferred choice for the following reasons:

1. Plotting measured flow data in the format of $\bar{u}_G$ versus <U>, as shown in Figure 17.10, yields linear (or nearly linear) representations of the data for a particular type of flow pattern. This was known empirically to be the case, and then Zuber and Findley arrived at the reason for this linear relationship analytically with [17.4.8]. Hence, analysis of experimental data can yield values of

C_o (the slope) and $\bar{U}_{GU}$ (the y-intercept) for different types of flow patterns using [17.4.8]. Note that homogeneous flow gives the diagonal straight line dividing adiabatic upflow from adiabatic downflow.

2. Various profiles can be assumed for integrating [17.4.23] and hence appropriate values of C_o can be derived for different flow patterns and specific operating conditions (e.g. high reduced pressures) in a systematic manner.

3. As a general approach, the drift flux model provides a unified approach to representing void fractions. It is capable of being applied to all directions of flow (upward, downward, horizontal and inclined) and potentially to all the types of flow patterns.

4. Reviewing of the expressions for $\bar{U}_{GU}$, the drift flux model includes the important effects of mass velocity, viscosity, surface tension and channel size as needed, which are missing in most other analytical methods.

17.6 Void Fraction in Shell-Side Flows on Tube Bundles

Void fractions in two-phase flows over tube bundles are much more difficult to measure than for internal channel flows and thus much less attention has been addressed to this flow geometry. Mass velocities of industrial interest also tend to be much lower than for internal flows. For evaporation and condensation on tube bundles in refrigeration systems, for instance, typical design mass velocities are in the range from 5 to 40 kg/m^{2}s. These low mass velocities are the result of the type of design utilized for these heat exchangers, that is simple cross flow entering from below or from above the bundle for flooded evaporators and for condensers, respectively. In partial evaporators and condensers common to the chemical processing industry with single segmental baffles, the normal design range is higher and ranges from about 25 to 150 kg/m^{2}s. This is still below much of the range confronted in tube-side evaporators and condensers (about 75 to 500 kg/m^{2}s). As a consequence, for vertical two-phase flows across tube bundles the frictional pressure drop tends to be small compared to the static head of the two-phase fluid. Therefore, the void fraction becomes the most important parameter for evaluating the two-phase pressure drop since it is directly related to the local two-phase density of the shell-side flow. Thus, even though shell-side void fractions have been studied less than internal channel flows, they are still very important for obtaining accurate thermal designs. In particular, for horizontal thermosyphon reboilers for instance, the circulation rate depends directly on the two-phase pressure drop across the tube bundle and hence the variation in void fraction is of primary importance. Furthermore, in flooded type evaporators with close temperature approaches in refrigeration and heat pump applications, the effect of the two-phase pressure drop on the saturation temperature may be significant in evaluating the log mean temperature difference of these units.

17.6.1 Vertical Two-Phase Flows on Tube Bundles

The earliest study was apparently that of Kondo and Nakajima (1980) who investigated air-water mixtures in vertical upflow for staggered tube layouts. They utilized quick-closing valves at the inlet and outlet of the bundle that included not only the tube bundle but also the entrance and exit zones. Based on the mass of liquid in the bundle, the void fraction was determined. Their tests covered qualities from 0.005 to 0.90 with mass velocities of 10 to 60 kg/m^{2}s, where the mass velocity as standard practice is evaluated at the minimum cross section of the bundle similar to single-phase flow. They found that the void fraction increased with superficial gas velocity while the superficial liquid velocity had almost no affect on void fraction. Notably, they observed that the number of tube rows had an effect on void fraction, but this probably resulted from their inclusion of the inlet and exit zones when measuring void

fractions. It should be noted here that the quick-closing valve technique yields *volumetric* void fractions, which are only equal to *cross-sectional* void fractions (i.e. those described in most of this chapter) when S = 1; when S >1, the volumetric void fraction is larger than the cross-sectional void fraction.

Schrage et al. (1988) made similar tests with air-water mixtures on inline tube bundles with a tube pitch to diameter ratio of 1.3, again using the quick-closing valve technique, ran tests for qualities up to 0.65, pressures up to 0.3 MPa and mass velocities from 54 to 683 kg/m^{2}s. At a fixed quality x, the volumetric void fraction was found to increase with increasing mass velocity. They offered a dimensional empirical relation for predicting volumetric void fractions by applying a multiplier to the homogeneous void fraction, the latter referred to here as ε_H. A non-dimensional version was obtained using further refrigerant R-113 data and it is as follows:

$$\frac{\varepsilon_{vol}}{\varepsilon_H} = 1 + 0.123\left(\frac{\ln x}{Fr_L^{0.191}}\right) \qquad [17.6.1]$$

Their liquid Froude number is based on the outside tube diameter D and was defined as:

$$Fr_L = \frac{\dot{m}}{\rho_L (gD)^{1/2}} \qquad [17.6.2]$$

According to Burnside et al. (1999), the above expression worked reasonably well in predicting their n-pentane two-phase pressure drop data together with the Ishihara et al. (1980) two-phase multiplier for tube bundles (although the *cross-sectional* void fraction should be used for calculating static pressure drops in two-phase flows, not the *volumetric* void fraction). Their tests were for a 241-tube bundle with an inline tube layout, a 25.4 mm pitch and 19.05 mm diameter tubes. Schrage et al. placed the following restriction on the above equation: when the void fraction ratio ($\varepsilon_{vol}/\varepsilon_H$) is less than 0.1, then a value of ($\varepsilon_{vol}/\varepsilon_H$) equal to 0.1 should be used.

Chisholm (1967) proposed a simple representation of the Lockhart and Martinelli (1949) method with a factor C to represent their graphical relationship of the liquid and vapor flows (laminar or turbulent), where C = 20 for both phases turbulent. Based on two-phase pressure drop data on tube bundles, Ishihara et al. (1980) found that using C = 8 gave the best representation as long as the Martinelli parameter satisfied $X_{tt} < 0.2$. The following curvefit gives an expression for void fraction from the Lockhart and Martinelli graphical method:

$$\varepsilon = 1 - \frac{1}{\phi_L} \qquad [17.6.3]$$

Here the local void fraction for flow over tube bundles is based on the two-phase friction multiplier of the liquid ϕ_L, which is given as:

$$\phi_L = 1 + \frac{8}{X_{tt}} + \frac{1}{X_{tt}^2} \qquad [17.6.4]$$

using the value of C = 8 and where X_{tt} is the Martinelli parameter for both phases in turbulent flow *across the bundle*. Determined with an appropriate shell-side friction factor expression, this expression reduces to the simplified form

$$X_{tt} = \left(\frac{1-x}{x}\right)\left(\frac{\rho_G}{\rho_L}\right)^{0.57}\left(\frac{\mu_L}{\mu_G}\right)^{0.11} \qquad [17.6.5]$$

Similarly, Fair and Klip (1983) offered a method for horizontal reboilers used in the petrochemical industry:

$$(1-\varepsilon)^2 = \frac{1}{\phi_L} \qquad [17.6.6]$$

Their liquid two-phase friction multiplier ϕ_L is given by

$$\phi_L = 1 + \frac{20}{X_{tt}} + \frac{1}{X_{tt}^2} \qquad [17.6.7]$$

where X_{tt} for both fluids turbulent is the same as above.

Rather than trying to find a Martinelli parameter based method to predict void fraction, Feenstra, Weaver and Judd (2000) concentrated on developing a completely empirical expression to predict the velocity ratio S, where the eventual expression for S should obey the correct limits at vapor qualities of 0 and 1. For their dimensional analysis approach, they identified the following functional parameters as influencing S: two-phase density, liquid-vapor density difference, pitch flow velocity of the fluid, dynamic viscosity of the liquid, surface tension, gravitational acceleration, the gap between neighboring tubes, tube diameter, tube pitch and the frictional pressure gradient. The two-phase density and density difference were included as they are always key parameters in void fraction models. The tube pitch L_{tp} and tube diameter D were included for their influence on the frictional pressure drop. Furthermore, the surface tension σ was selected since it affects the bubble size and shape and the liquid dynamic viscosity μ_L was included because of its affect on bubble rise velocities. This approach resulted in the following void fraction prediction method:

$$\varepsilon = \frac{1}{1 + S\left(\frac{(1-x)}{x}\frac{\rho_G}{\rho_L}\right)} \qquad [17.6.8]$$

where the velocity (or slip) ratio S is calculated as:

$$S = 1 + 25.7\,(\text{Ri Cap})^{0.5}\left(L_{tp}/D\right)^{-1} \qquad [17.6.9]$$

In this expression, L_{tp}/D is the tube pitch ratio and the Richardson number Ri is defined as:

$$\text{Ri} = \frac{(\rho_L - \rho_G)^2\, g\left(L_{tp} - D\right)}{\dot{m}^2} \qquad [17.6.10]$$

The Richardson number represents a ratio between the buoyancy force and the inertia force. The mass velocity, as in all these methods for tube bundles, is based on the minimum cross-sectional flow area like

in single-phase flows. The characteristic dimension is the gap between the tubes, which is equal to the tube pitch less the tube diameter, L_{tp}-D. The Capillary number Cap is defined as:

$$Cap = \frac{\mu_L u_G}{\sigma} \qquad [17.6.11]$$

The Capillary number represents the ratio between the viscous force and the surface tension force. The mean vapor phase velocity u_G is determined based on the resulting void fraction as

$$u_G = \frac{x\dot{m}}{\varepsilon\rho_G} \qquad [17.6.12]$$

Hence, an iterative procedure is required to determine the void fraction using this method. This method was successfully compared to air-water, R-11, R-113 and water-steam void fraction data obtained from different sources, including the data of Schrage, Hsu and Jensen (1988). It was developed from triangular and square tube pitch data with tube pitch to tube diameter ratios from 1.3 to 1.75 for arrays with from 28 to 121 tubes and tube diameters from 6.35 to 19.05 mm. Their method was also found to be the best for predicting static pressure drops at low mass flow rates for an 8-tube row high bundle under evaporating conditions (where the accelerated and frictional pressure drops were relatively small) by Consolini, Robinson and Thome (2006). Hence, the Feenstra-Weaver-Judd method is thought to be the most accurate and reliable available for predicting void fractions in vertical two-phase flows on tube bundles.

Example 17.5: Determine the void fraction and velocity ratio using the Feenstra-Weaver-Judd method at a vapor quality of 0.2 for R-134a at a saturation temperature of 4°C (3.377 bar) for a mass velocity of 30 kg/m^{2}s, a tube diameter of 19.05 mm (3/4 in.) and tube pitch of 23.8125 mm (15/16 in.). The properties required are: ρ_L = 1281 kg/m^3; ρ_G = 16.56 kg/m^3; σ = 0.011 N/m; μ_L = 0.0002576 Ns/m^2.

Solution: The calculation starts by assuming a value for the void fraction, which in this case the value of 0.5 is taken as the starting point in the iterative procedure. First, the mean vapor velocity is determined to be:

$$u_G = \frac{0.2(30)}{0.5(16.56)} = 0.725\,\text{m/s}$$

Next the Capillary number is determined:

$$Cap = \frac{0.0002576(0.725)}{0.011} = 0.0170$$

The Richardson number Ri is determined next:

$$Ri = \frac{(1281-16.56)^2\,(9.81)(0.0238125-0.01905)}{30^2} = 83.0$$

The velocity (or slip) ratio S is then calculated:

$$S = 1 + 25.7\left[83.0(0.0170)\right]^{0.5}(0.0238125/0.01905)^{-1} = 25.4$$

The void fraction is then:

$$\varepsilon = \frac{1}{1 + 25.4\left(\frac{(1-0.2)}{0.2}\frac{16.56}{1281}\right)} = 0.432$$

The second iteration begins using this value to determine the new mean vapor velocity and so on until the calculation converges. After 6 iterations, ε becomes 0.409 (with an error of less than 0.001).

17.6.2 Horizontal Two-Phase Flows on Tube Bundles

Grant and Chisholm (1979), using air-water mixtures, investigated void fractions in horizontal crossflow in a baffled heat exchanger with four crossflow zones and three window areas (note: a window refers to where the flow goes through the baffle cut and where it is hence longitudinal to the tubes rather than across the tubes). They studied stratified flows and measured the liquid levels in the first and fourth baffle compartments, noting that the void fraction was less in the first baffle compartment with respect to the fourth compartment for all mass velocities tested. They proposed the following correlation for void fraction:

$$1 - \varepsilon = \frac{1}{1 + \left(\frac{x}{1-x}\right)\left(\frac{\rho_L}{\rho_G}\right)\left(\frac{1}{S}\right)} \qquad [17.6.13]$$

The empirical factor S is a velocity ratio evaluated as

$$S = \left(\frac{\mu_L}{\mu_G}\right)^{\frac{m}{2-m}}\left(\frac{\rho_L}{\rho_G}\right)^{\frac{1-m}{2-m}} \qquad [17.6.14]$$

where m is obtained by fitting the method to experimental data. They noted that this method worked well at low qualities but overestimated the measured void fractions at higher qualities.

Xu, Tou and Tso (1998) also proposed a separated flow approach based loosely on the Lockhart and Martinelli (1949) separated flow model to tube-side flow, extrapolating the equations to flow over tube-bundles where their X_{tt} is the Martinelli parameter given by:

$$X_{tt} = \left(\frac{1-x}{x}\right)^{0.9}\left(\frac{\rho_G}{\rho_L}\right)^{0.5}\left(\frac{\mu_L}{\mu_G}\right)^{0.1} \qquad [17.6.15]$$

They proposed the following void fraction expression:

$$\frac{\varepsilon}{1-\varepsilon} = a_1 Fr_L^{a_2} X_{tt}^{-a_3} \qquad [17.6.16]$$

The constants $a_1 = 1.95$, $a_2 = 0.18$, and $a_3 = 0.833$ gave the best fit to their air-water and air-oil data. Their Froude number was defined as:

$$Fr_L = \frac{\dot{m}^2}{\rho_L^2 gD} \qquad [17.6.17]$$

Their Froude number is the squared value of that used in the Schrage et al. method above and D is the outside tube diameter.

Figure 17.11 illustrates a graphic comparison of the predictions for four different void fraction models presented in this chapter. At a given vapor quality, the homogeneous model gives the highest value for the void fraction, while the Feenstra-Weaver-Judd model predicts the lowest.

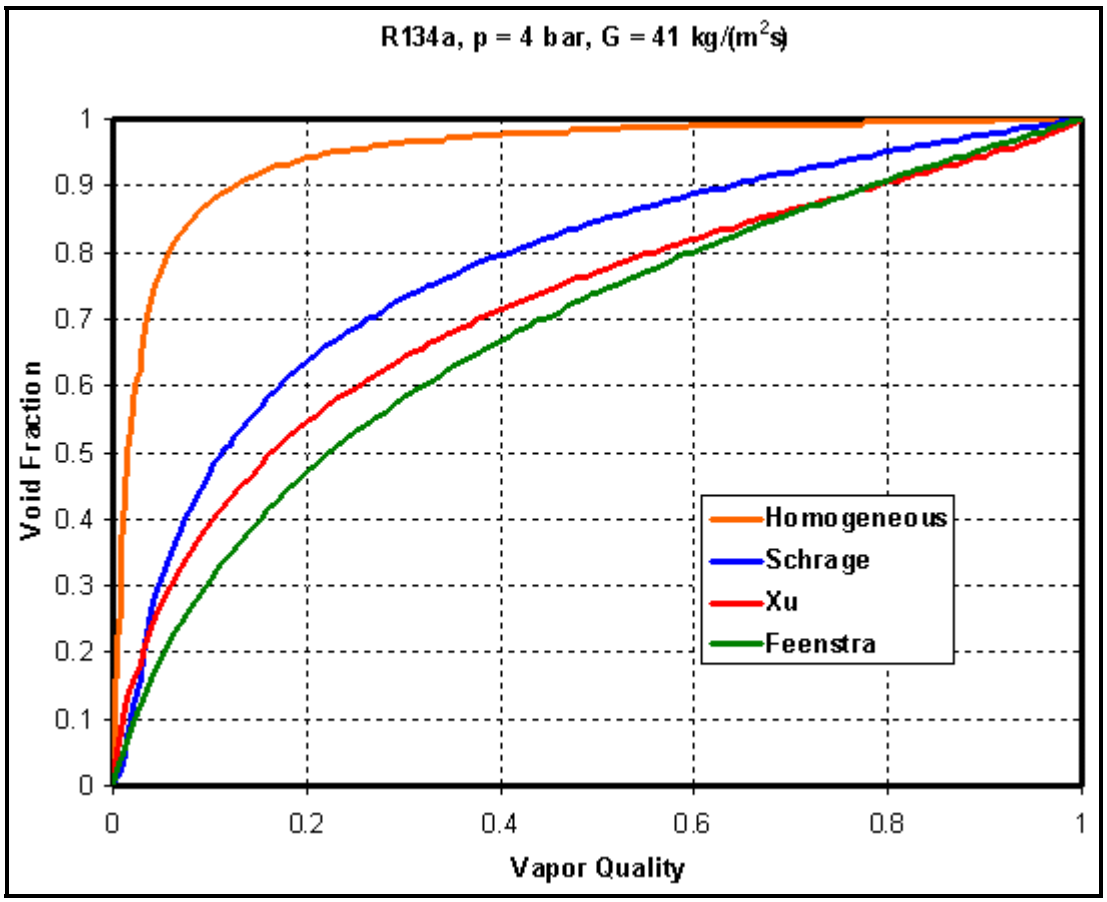

Figure 17.11. Comparison of select bundle void fraction methods for R-134a at 0.4 MPa for 19.05 mm tubes on a 22.2 mm triangular pitch.

Example 17.6: A laminar stratified liquid-vapor mixture is flowing between two horizontal flat plates. Evaluate the slip ratio given a measured void fraction of $\varepsilon = 0.6$. Assume both phases to be in steady fully developed conditions. The fluid is saturated water at 33°C ($\mu_L = 750$ μPa s, $\mu_G = 10$ μPa s, $\rho_L = 995$ kg/m^3, $\rho_G = 0.034$ kg/m^3). Compare this value to those obtained from the momentum flux model, eq. [17.3.4], and the Zivi model, eq. [17.3.13].

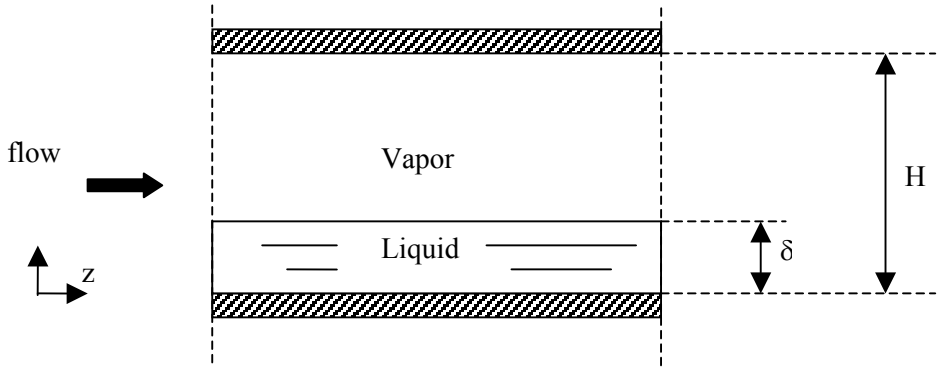

Solution: The two-phase system is shown in the following figure, where δ represents the constant thickness of the liquid layer.

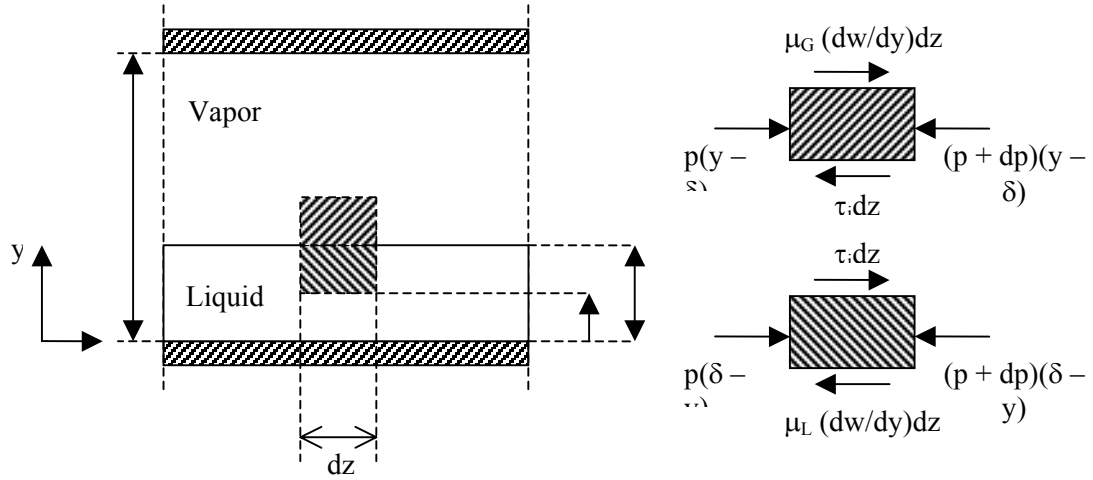

Performing a mass balance on the control volumes shown above yields the following expressions for the liquid and vapor, respectively (using v as the velocity component in the y-direction, w as the velocity component in the z-direction and W as the average cross-sectional velocity in the z-direction):

$$v(y,z) - v(\delta^-,z) = \int_y^\delta \frac{\partial w}{\partial z}\,dy$$

$$v(y,z) - v(\delta^+,z) = -\int_\delta^y \frac{\partial w}{\partial z}\,dy$$

For the fully developed flow w = w(y); therefore the terms on the right hand sides of the above equations are set equal to zero. Neglecting any mass transfer provides the boundary condition:

$$v(\delta^-,z) = v(\delta^+,z) = 0$$

Consequently, the orthogonal component of the velocity field is equal to zero in the entire domain, so that

$$v(y,z) = 0$$

Applying this to a momentum balance in the y direction gives:

$$p(y,z) = p(\delta^-,z)$$

$$p(y,z) = p(\delta^+,z)$$

for $0 \le y \le \delta$ and $\delta \le y \le H$, respectively. The vertical force balance at the interface (i.e. $p(\delta^-,z) = p(\delta^+,z)$) results in a constant pressure over any cross-section. In mathematical terms:

$$p = p(z)$$

Momentum transport in the flow direction yields the following set of equations for the liquid and vapor phases, respectively:

$$0 = -\frac{dp}{dz}(\delta - y)dz + \tau_i dz - \mu_L \frac{dw}{dy}dz$$

$$0 = -\frac{dp}{dz}(y - \delta)dz - \tau_i dz + \mu_G \frac{dw}{dy}dz$$

The inertial terms that would normally appear on the left-hand sides of the two equations are set to 0 since the flow is fully developed and v = 0. The interfacial shear τ_i is related to the velocity gradients in both phases by:

$$\tau_i = \mu_L \left.\frac{dw}{dy}\right|_{\delta^-} = \mu_G \left.\frac{dw}{dy}\right|_{\delta^+}$$

It is therefore either constant or simply a function of y. From this remark it follows that the pressure gradient term appearing in the two momentum equations will have to be a constant. After some rearrangement and setting the boundary conditions, one obtains:

$$\begin{cases} \dfrac{dw}{dy} = -\dfrac{1}{\mu_L}\dfrac{dp}{dz}(\delta - y) + \dfrac{\tau_i}{\mu_L} & 0 \le y < \delta \\ \dfrac{dw}{dy} = \dfrac{1}{\mu_G}\dfrac{dp}{dz}(y - \delta) + \dfrac{\tau_i}{\mu_G} & \delta \le y < H \\ w(\delta^-) = w(\delta^+) = 0 & \\ w(y = 0) = 0 & \\ w(y = H) = 0 & \end{cases}$$

The velocity profiles for the two phases are given by integrating the two ordinary differential equations by separation of variables and applying the no-slip condition at the wall:

$$w(y) = \frac{1}{2\mu_L}\frac{dp}{dz}\left[(\delta - y)^2 - \delta^2\right] + \frac{\tau_i}{\mu_L}y \qquad 0 \le y < \delta$$

$$w(y) = \frac{1}{2\mu_G}\frac{dp}{dz}\left[(y - \delta)^2 - (H - \delta)^2\right] + \frac{\tau_i}{\mu_G}(y - H) \qquad \delta \le y < H$$

At the interface the two values of w must be equal, that is:

$$-\frac{1}{2\mu_L}\frac{dp}{dz}\delta^2 + \frac{\tau_i}{\mu_L}\delta = -\frac{1}{2\mu_G}\frac{dp}{dz}(H - \delta)^2 - \frac{\tau_i}{\mu_G}(H - \delta)$$

Rearranging this equation and observing that $\delta = H(1 - \varepsilon)$ yields:

$$\frac{dp}{dz} = \left[\frac{2}{H}\frac{\mu_G(1-\varepsilon) + \mu_L\varepsilon}{\mu_G(1-\varepsilon)^2 - \mu_L\varepsilon^2}\right]\tau_i$$

The velocity profiles for the two phases are shown in the following figure. The computation of the slip ratio requires the average velocities of the two phases. For the liquid:

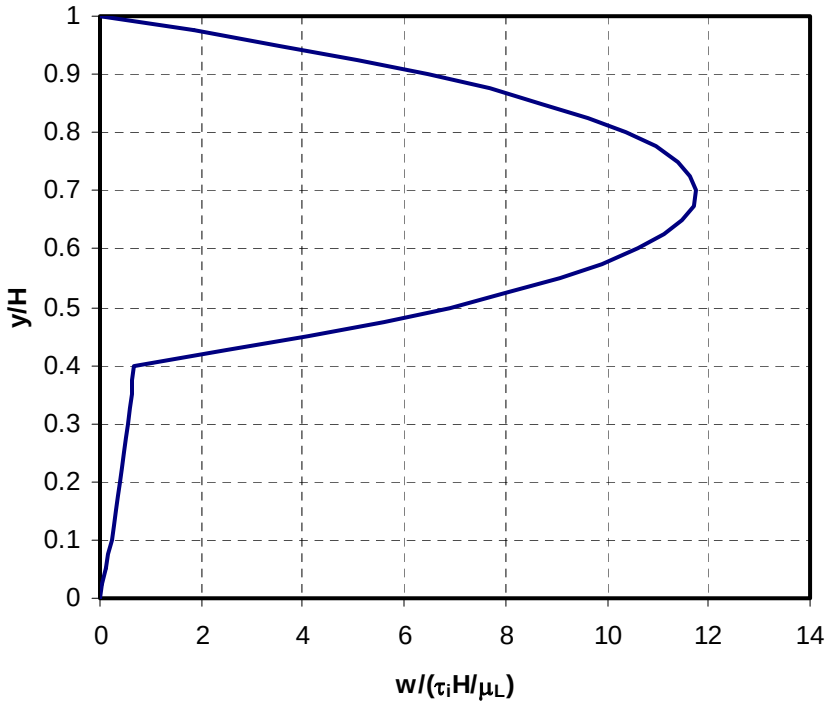

$$W_L = \frac{1}{\delta}\int_0^{\delta}\left\{\frac{1}{2\mu_L}\frac{dp}{dz}\left[(\delta - y)^2 - \delta^2\right] + \frac{\tau_i}{\mu_L}y\right\}dy$$

After integration, the average velocity of the liquid phase is given as follows:

$$W_L = \frac{\delta}{2\mu_L}\left(\tau_i - \frac{2}{3}\frac{dp}{dz}\delta\right)$$

In the same way for the vapor phase:

$$W_G = \frac{1}{H-\delta}\int_{\delta}^{H}\left\{\frac{1}{2\mu_G}\frac{dp}{dz}\left[(y-\delta)^2 - (H-\delta)^2\right] + \frac{\tau_i}{\mu_G}(y-H)\right\}dy$$

Integrating:

$$W_G = \frac{H-\delta}{2\mu_G}\left[-\tau_i - \frac{2}{3}\frac{dp}{dz}(H-\delta)\right]$$

From the definition of the slip ratio, S:

$$S = \frac{W_G}{W_L} = -\frac{\mu_L}{\mu_G}\frac{\varepsilon}{1-\varepsilon}\left[\frac{\tau_i + \frac{2}{3}\frac{dp}{dz}H\varepsilon}{\tau_i - \frac{2}{3}\frac{dp}{dz}H(1-\varepsilon)}\right]$$

Using the previously derived expression for the pressure gradient,

$$\frac{dp}{dz} = \left[\frac{2}{H}\frac{\mu_G(1-\varepsilon)+\mu_L\varepsilon}{\mu_G(1-\varepsilon)^2 - \mu_L\varepsilon^2}\right]\tau_i$$

S becomes a function only of the void fraction and the viscosity ratio:

$$S = \left(\frac{\mu_L}{\mu_G}\right)^2\frac{\varepsilon}{1-\varepsilon}\left[\frac{\frac{1}{3}\varepsilon^2 + \frac{4}{3}\frac{\mu_G}{\mu_L}\varepsilon(1-\varepsilon) + \frac{\mu_G}{\mu_L}(1-\varepsilon)^2}{\frac{\mu_L}{\mu_G}\varepsilon^2 + \frac{4}{3}\frac{\mu_L}{\mu_G}\varepsilon(1-\varepsilon) + \frac{1}{3}(1-\varepsilon)^2}\right] = 20.9$$

This value differs substantially from the momentum flux model:

$$S_{\text{momentum flux}} = \left(\frac{\rho_L}{\rho_G}\right)^{1/2} = 171$$

On the other hand, it is in better agreement with the prediction of Zivi:

$$S_{Zivi} = \left(\frac{\rho_L}{\rho_G}\right)^{1/3} = 30.8$$

Homework Problems:

17.1: Determine the void fraction for the following vapor qualities (0.01, 0.1 and 0.25) using the following methods: homogeneous flow, momentum flux model and both of Zivi's expressions. The liquid density is 1200 kg/m^3 and the gas density is 200 kg/m^3. Assume the liquid entrainment is equal to 0.4.

17.2: Determine the void fraction for a vapor quality of 0.1 using the second of Zivi's expressions using the properties above. Assume liquid entrainments equal to 0.0, 0.2, 0.4, 0.6, 0.8 and 1.0.

17.3: Determine the local void fractions using the Rouhani expressions [17.4.31] and [17.4.32] for the following qualities (0.1, 0.50, 0.95) for a fluid flowing at rates of 0.05 and 0.2 kg/s in a horizontal tube of 22 mm internal diameter for the same conditions as in Example 17.4. Compare and comment. The surface tension is 0.012 N/m.

17.4: Determine the local void fraction using the drift flux model assuming bubbly flow for the following qualities (0.01, 0.05, 0.1) for a fluid flowing at a rate of 0.5 kg/s in a vertical tube of 40 mm internal diameter. The fluid has the following physical properties: liquid density is 1200 kg/m^3, gas density is 20 kg/m^3 and surface tension is 0.012 N/m.

17.5: Determine the local void fraction using the drift flux model assuming slug flow for the following qualities (0.05, 0.1) for the same conditions as in Problem 17.4.

17.6: Determine the local void fraction using the drift flux model assuming annular flow at a quality of 0.5 for a fluid flowing at a rate of 0.5 kg/s in a vertical tube of 40 mm internal diameter. The fluid has the following physical properties: liquid density is 1000 kg/m^3, gas density is 50 kg/m^3, surface tension is 0.05 N/m and the liquid dynamic viscosity is 0.0006 Ns/m^2.

17.7: Determine the local void fractions using the method of Ishihara et al. for the following qualities (0.05, 0.1, 0.50) at a mass velocity of 100 kg/m^{2}s flowing across a tube bundle with tubes of 25.4 mm outside diameter. The fluid has the following physical properties: liquid density is 1200 kg/m^3, gas density is 20 kg/m^3, surface tension is 0.012 N/m and the liquid and vapor dynamic viscosities are 0.0003 Ns/m^2 and 0.00001 Ns/m^2.

17.8: Determine the local void fractions using the method of Fair and Klip for the same conditions as in Problem 17.7.

17.9: Derive expression [17.3.13] from [17.3.12].

17.10: Derive Zivi's second void fraction expression with entrained liquid in the gas phase, i.e. expression [17.3.15].

17.11: Derive expressions [17.4.26] and [17.4.27].